**Journal of Biomolecular Structure and Dynamics**

Taylor & Francis
Taylor & Francis Group

# Molecular investigation of artificial and natural sweeteners as potential anti-inflammatory agents

Eleni Chontzopoulou, Christina D. Papaemmanouil, Maria V. Chatziathanasiadou, Dimitrios Kolokouris, Sofia Kiriakidi, Athina Konstantinidi, Ioanna Gerogianni, Theodore Tselios, Ioannis K. Kostakis, Evangelia D. Chrysina, Dimitra Hadjipavlou-Litina, Demeter Tzeli, Andreas G. Tzakos & Thomas Mavromoustakos

| | |
|---|---|
| View supplementary material ⧉ | Published online: 09 Sep 2021. |
| Submit your article to this journal ⧉ | Article views: 217 |
| View related articles ⧉ | View Crossmark data ⧉ |
| Citing articles: 3 View citing articles ⧉ | |

Taylor & Francis
Taylor & Francis Group

Check for updates

# Molecular investigation of artificial and natural sweeteners as potential anti-inflammatory agents

Eleni Chontzopoulou[a], Christina D. Papaemmanouil[b], Maria V. Chatziathanasiadou[b], Dimitrios Kolokouris[c], Sofia Kiriakidi[a], Athina Konstantinidi[c], Ioanna Gerogianni[d,e], Theodore Tselios[f], Ioannis K. Kostakis[c], Evangelia D. Chrysina[d,e], Dimitra Hadjipavlou-Litina[a], Demeter Tzeli[a], Andreas G. Tzakos[b,g] and Thomas Mavromoustakos[a]

[a]Department of Chemistry, National and Kapodistrian University of Athens, Athens, Greece; [b]Department of Chemistry, Section of Organic Chemistry and Biochemistry, University of Ioannina, Ioannina, Greece; [c]Department of Pharmacy, National and Kapodistrian, University of Athens, Athens, Greece; [d]Institute of Biology, Medicinal Chemistry and Biotechnology, Department of Pharmaceutical Chemistry, School of Pharmacy, Faculty of Health Sciences, National Hellenic Research Foundation, Athens, Greece; [e]Department of Pharmacy, Aristotle University of Thessaloniki, Thessaloniki, Greece; [f]Department of Chemistry, University of Patras, Rion, Greece; [g]Institute of Materials Science and Computing, University Research Center of Ioannina (URCI), Ioannina, Greece

Communicated by Ramaswamy H. Sarma

## ABSTRACT

Repurposing existing drugs, as well as natural and artificial sweeteners for novel therapeutic indications could speed up the drug discovery process since numerous associated risks and costs for drug development can be surpassed. In this study, natural and artificial sweeteners have been evaluated by *in silico* and experimental studies for their potency to inhibit lipoxygenase enzyme, an enzyme participating in the inflammation pathway. A variety of different methods pinpointed that aspartame inhibits the lipoxygenase isoform 1 (LOX-1). In particular, "LOX-aspartame" complex, that was predicted by docking studies, was further evaluated by Molecular Dynamics (MD) simulations in order to assess the stability of the complex. The binding energy of the complex has been calculated after MD simulations using Molecular Mechanics/Generalized Born Surface Area (MM/GBSA) method. Furthermore, Quantum Mechanics/Molecular Mechanics (QM/MM) calculations have been applied for geometry optimization of the "enzyme-ligand" complex. After having fully characterized the "LOX-aspartame" complex *in silico*, followed *in vitro* biological assays confirmed that aspartame inhibits LOX-1 (IC$_{50}$=50±3.0 μM) and blocks its biological response. The atomic details of aspartame's interaction profile with LOX-1 were revealed through Saturation Transfer Difference (STD) NMR (Nuclear Magnetic Resonance). Finally, aspartame was also tested with Molecular Docking and Molecular Dynamics studies for its potent binding to a number of different LOX isoforms of many organisms, including human. The *in silico* methods indicated that aspartame could serve as a novel starting point for drug design against LOX enzyme.
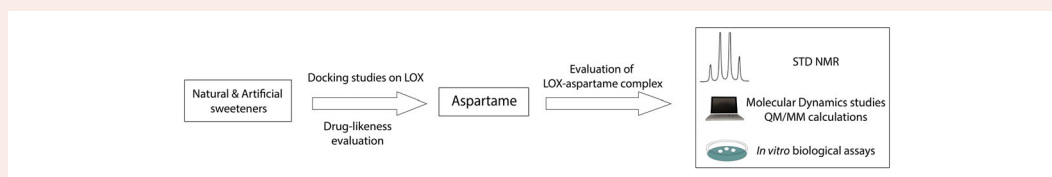
## 1. Introduction

Inflammation is the biological response of human's tissues against any type of harmful stimulus. The biochemical pathway of inflammation is characterized by the presence of three enzymes responsible for the creation of inflammatory agents in the cell: human cytosolic phospholipase A2 (cPLA2), cyclooxygenase (COX) and lipoxygenase (LOX) (Khanapure & Gordon Letts, 2004). Cycloxygenase superfamily has been thoroughly investigated and many COX-1 and COX-2 inhibitors are commercially available, such as aspirin (Flower, 2003) and NSAIDs (Rouzer & Marnett, 2009), while there is only one commercially available inhibitor targeting lipoxygenase enzyme. Despite the fact that LOXs' crystal structures have been revealed since decades and the association of their metabolites with a variety of diseases has been established, there is only one commercially available inhibitor targeting human 5-LOX (zileuton/ABT-671) which is administrated for the treatment of asthma (Carter et al., 1991). Zileuton presents high liver toxicity and short half-life time,

hence the need to discover novel LOX inhibitors with improved pharmacokinetics and pharmacodymamic profile is a significant priority (Valentovic, 2007).

Lipoxygenase metabolizes arachidonic acid (AA) and produces an array of compounds, such as leukotrienes (A4, B4, C4, etc.) and lipoxins (Murphy & Gijon, 2007). In particular, LOX superfamily catalyzes the regio- and stereospecific dioxygenation of polyunsaturated fatty acids (PUFAs), containing a (1Z,4Z)- penta-1,4-diene system, leading to the production of hydroperoxy derivatives (Brash, 1999). The implication of these metabolites in inflammatory pathways is unambiquously related to the development of numerous different pathological diseases, such as asthma (Mashima & Okuyama, 2015), atherosclerosis (Feinmark & Cornicelli, 1997; Rioux & Castonguay, 1998), rheumatoid arthritis (Gheorghe et al., 2009), psoriasis (Dobrian et al., 2011), brain disorders (Karatas & Cakir-Aktas, 2019; Praticò et al., 2004) and cancer (Avis et al., 1996; Catalano & Procopio, 2005; Claria & Romano, 2005; Haeggström & Funk, 2011; Rioux & Castonguay, 1998). Moreover, LOXs have been reported to possess tumor promoting properties, while their products, leukotriene LTB4, can lead to the activation of the NF-Kb, a master regulator of inflammation processes in the tumor microenvironment (Zhao et al., 2012). Furthermore, human 5-LOX has been found overexpressed in pancreatic neoplastic lesions and thus targeting lipoxygenases has been emerged as an alternative method to suppress inflammation and tumor development.

LOXs' main structure is monomeric and it consists of a C2 β-barrel domain (region connecting to the lipid bilayers of the cell) and an α-helix catalytic domain containing the active site of the protein (Boyington et al., 1990). The architecture of active site is characterized by the Fe atom coordinated by 3 histidine residues and one C-terminal isoleucine, while the other ligands coordinating Fe cation vary among LOX isoforms (Choi et al., 2008; Gilbert et al., 2020; Offenbacher et al., 2017; Xu et al., 2012).

Recently, the concept of "drug repurposing" has gained ground since it promotes the discovery of novel uses for approved drugs as a mean to deliver the quickest possible transition from bench to bedside (Oprea et al., 2011; Rana et al., 2019; Sharma et al., 2020). Food supplements and natural products have been also explored for their potent pharmaceutical properties. The discovery of special properties to such compounds may accelerate their commercial circulation, as they have already been assessed for their safety and toxicity. Various artificial high-intensity sweeteners such as acesulfame potassium, sucralose, neotame and advantame have been approved by the FDA as food or beverage additives (US Food & Drug Administration., n.d). Moreover, natural sweeteners have been extensively used in the last decades as sugar substitutes to a variety of foods and beverages, while they are also utilized as additives in pharmaceutics for masking drugs' taste (Gupta et al., 2017).

Until now, these molecules have been thoroughly studied in human and animal studies mainly for their impact in human health (Lim, 2016) and the results led virtually to their approval as safe for consumption (Magnuson et al., 2007). Recent studies reported that sweeteners such as sucralose or stevia affect positively the increase of flavonoids concentration in human plasma. It is of great concern that numerous flavonoids, phenolic acids, anthocyanidins and all their structural derivatives have been implicated in the treatment against various diseases, including cancer, and, thus, their presence in human plasma is vital (Agulló et al., 2021). In addition, it has also been found that natural sweeteners could act as protecting agents against oxidative stress, a crucial leader of DNA damage and cytotoxicity (Li et al., 2021). These widely-used sweeteners could be the pillars for the investigation concerning the health benefits that may provide and their implication in molecular mechanisms and subsequently their potential use as lead compounds. In this direction, acesulfame potassium and saccharin have been proved to inhibit selectively the carbonic anhydrase IX, an enzyme playing crucial role in the survival of tumor cells (Lomelino et al., 2018; Mahon et al., 2015; Murray et al., 1986). Moreover, sucralose reduces the VEGF-induced vasculogenesis in human retinal microvascular endothelial cells by activating the GPCR receptor T1R3 (Lizunkova et al., 2019).

Aspartame (Figure 1b), a methyl ester of the aspartic acid-phenylalanine dipeptide, is an artificial sweetener used as a sugar substitute in many edible products. Aspartame binds in the closed form of Venus Flytrap Module (VFTM) (Maillet et al., 2015) which is the active sweet human receptor TlR2 (hTlR2) and is approximately 200 times sweeter than sucrose (US Food & Drug Administration., n.d). Despite the controversy concerning the effects of aspartame in human health that had been raised in the past, the majority of the scientific studies have supported that the artificial sweetener is safe to consume while the acceptable daily uptake has been set up to 50 mg/kg by the FDA (US Food & Drug Administration., n.d).

In this study, all natural and artificial sweeteners have been evaluated in silico for their potency to exhibit anti-inflammatory properties and serve as LOX inhibitors. The most prominent "LOX-1-sweetener" complex that was generated by docking studies, was further assessed for its stability through Molecular Dynamics and Quantum Mechanics/Molecular Mechanics calculations. All the in silico and experimental studies of natural and artificial sweeteners have been performed to soybean LOX-1 isoform, thus this enzyme could play the role-model for drug design against all isoforms of LOX superfamily. After having established compounds' inhibitory activity against LOX-1, in silico studies have been perfomed to other LOX isoforms in order to evaluate the compounds' activity towards different LOXs and investigate if LOX-1 could be the prototype for anti-LOX drug design process. Finally, in vitro assays verified the in silico findings and they indicated that aspartame is able to inhibit LOX-1, while the molecular interaction profile of the inhibition was unveiled with STD NMR experiments.

Currently, other lipoxygenase inhibitors have been also evaluated, such as atreleuton (Tardif et al., 2010) and diethyl-carbamazine (Zuo et al., 2004) that have been used for the treatment of atherosclerosis and filariasis, while licofelone (Cicero & Laghi, 2007) and masoprocol (Luo et al., 1998) act as dual COX/LOX inhibitors for the treatment of osteoarthritis and prostate cancer respectively (West et al., 2004). Even if
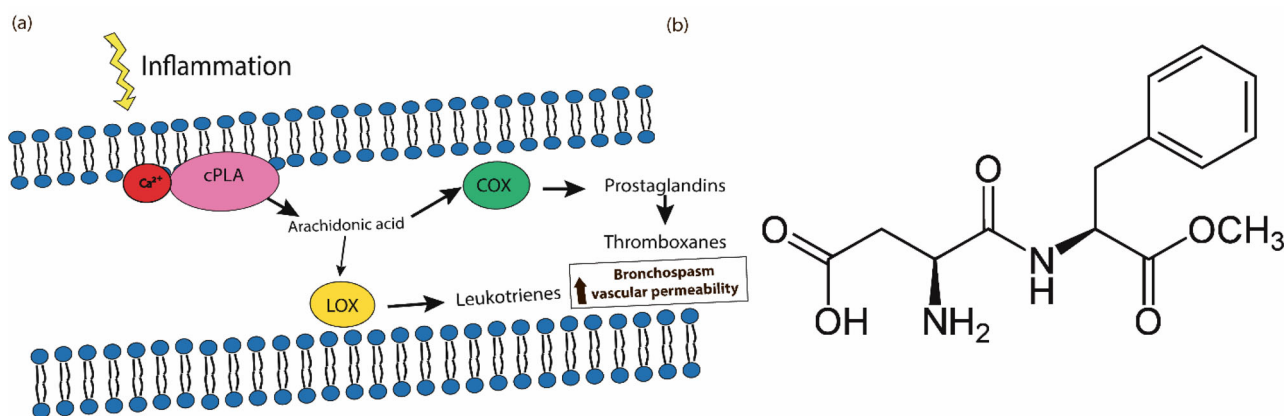
**Figure 1.** (a) Biochemical pathway of inflammation in human tissues. (b) Chemical structure of aspartame.

these LOX inhibitors are currently under investigation, there are no commercially available drugs targeting LOX, thus it is crucial to intensify the studies concerning the discovery of novel anti-LOX compounds and understand their linkage to severe diseases like cancer.

## 2. Materials and methods

### 2.1. Induced fit docking

The crystal structures used for the different LOX isoforms for the *in silico* studies were PDB IDs: 5T5V (Offenbacher et al., 2017), 3RDE (Xu et al., 2012), 3O8Y (Gilbert et al., 2011), 1LOX (Gillmor et al., 1997), 1RRH (Skrzypczak-Jankun et al., 2006), 3D3L, 4G32 (Garreta et al., 2013), 4NRE (Kobe et al., 2014), 5IR4 (Banthiya et al., 2016) and they were retrieved from Protein Data Bank (Protein Data Bank, 2021). Protein preparation wizard, module available in Schrödinger Suites (Schrödinger Maestro, 2018), was used to prepare the crystal structures for the *in silico* calculations. Since LOX is a metalloprotein, it has been taken into account that there are several computational challenges that need to be addressed. In order to account for the quantum effects associated with the presence of a $Fe^{3+}$ cation in the protein's active site, we used the "create zero-order bonds to metals" module of the Schrödinger's Maestro molecular modeling platform. This module breaks existing bonds to metals -since they cannot be examined through the oversimplified model of a spring attached to a hard sphere- adds new zero-order bonds between metals and nearby atoms and corrects their formal charges accordingly, in order to constrain the X-ray acquired coordination geometry.

The natural and artificial sweeteners' structures were prepared with LigPrep (Schrödinger LigPrep, 2018) module, while during the ligand preparation the "add metal binding states" option was chosen The geometries were optimized with MacroModel (Schrodinger, L.L.C, 2013) and the force field used was OPLS2005 (Jorgensen et al., 1996). Ligands were subjected to proper treatment of their protonation states at physiological pH (~7.4). The three-dimensional ligands' structures were further minimized, more rigorously, by MacroModel with water as solvent .The minimized structures were further used as input to a mixed-torsional/low-sampling conformational search forced to keep the input chiralities. The 10 most favored conformations were used as input for the following docking calculations (Schrodinger, 2015; Schrödinger LLC, 2011; Schrödinger LLC Prime, 2014; Sherman et al., 2006).

Docking calculations were performed with the Induced Fit Docking (IFD) method (Schrodinger, 2015). Protein preparation constrained refinement was applied in the Glide docking stage. Trimming side chains automatically (based on B – factor) and Prime (Schrödinger LLC Prime, 2014) refinement of the protein side chains were applied and the docking process was accomplished by Glide/XP (Schrödinger LLC, 2011). Finally, the binding energy for each ligand was calculated. The active site was described using a dielectric constant of 80 and all the crystallographic waters of the active site were preserved since the LOX's cavity should be hydrated. The same protocol was applied for all LOX isoforms.

### 2.2. Molecular dynamics

The system for the MD studies was setup with SPC/E modeled waters surrounding the drug-protein complex and neutralized with $Na^+$ and $Cl^-$ ions until the experimental salt concentration of 0.150 M NaCl was reached. The N- terminus of the protein was capped by an acetyl group, whereas the C-terminus remained uncapped since it is part of the protein's active site. The OPLS2005 force field was used to model all protein-ligand interactions and the long-range electrostatics were treated with the particle mesh Ewald method (PME) (Essmann et al., 1995; Martyna et al., 1994) and a grid spacing of 0.8 Å. Van der Waals and short-range electrostatic interactions were smoothly truncated at 9.0 Å. Temperature was kept constant using the Nosé-Hoover thermostat (Humphreys et al., 1994) while the Martyna-Tobias-Klein method (Martyna et al., 1994) was used to control the pressure. Periodic boundary conditions were applied and the dimensions of the simulation box were $(10.0 \times 10.0 \times 10.0)$ Å. The equations of motion were integrated using the multistep RESPA integrator (Lyman & Zuckerman, 2006) with an inner time step of 2 fs for bonded interactions and non-bonded interactions within a cutoff of 9 Å. An outer time step of 6.0 fs was used for non-bonded

interactions beyond the cut-off. Each system was equilibrated using the default protocol provided by Desmond (Version, 2021). The system was relaxed initially with Brownian dynamics simulation in the NVT ensemble at $T = 310$ K with restraints on solute heavy atoms. Before commencing with the production phase, the system was left to relax in the NPT ensemble with no restraints for 1.0 ns. The production phase of the MD simulation was set to 200 ns, which provides with an adequate sample size in order to analyze the binding mode of the molecule to protein's cavity.

The MD simulations were run in workstations using the GPU implementation of the MD simulations codes and the statistics of our simulation were evaluated based on the RMSD convergence of the protein backbone Cα atoms and the RMSD of the ligand.

All MD simulations have been performed three times to verify the reproducibility of the results and the trajectory has been analyzed with the Desmond and VMD Trajectory Analysis Tools.

## 2.3. Molecular Mechanics/generalized born surface area (MM/GBSA)

MM/GBSA was used to examine protein-ligand complexes to calculate free binding energy. MM/GBSA equations were extended to complex structures using the Prime module of Maestro. The three statistically predominant ligand-protein complexes that derived from MD trajectory cluster analysis were subjected to MM/GBSA calculations. VSGB solvation model (Schrödinger LigPrep, 2018) which is realistic parametrization of the solvation and OPLS-2005 forcefield were used for protein flexibility (Pattar et al., 2020).

## 2.4. Quantum mechanics/molecular mechanics calculations

The LOX-inhibitor complex was optimized at the hybrid QM/MM level using the QSite program which couples the Jaguar and Impact programs of the Schrödinger package. The QM part of the model consisted of 137 atoms from enzyme's residues Ile839, His504, His499, Asn694, His690, $H_2O1045$ and $Fe^{+3}$ ion, and of atoms of the bound inhibitor. For the QM part, the DFT methodology was used, applying the meta hybrid Minnesota functional with double the amount of nonlocal exchange (M06-2X) with the Los Alamos national laboratory effective core potential (LACVP*) basis set. The M06-2X functional was chosen based on previous studies on metalloproteins carrying a metal in the active site. The MM part of the system was treated with the OPLS2005 force field with no cut-offs introduced for nonbonding interactions, and the energy was minimized using the Truncated Newton Conjugate Gradient (TNCG) method. Convergence criterion is based on energy change ($1.0 \times 10^{-7}$ kcal/mol) and gradient (0.01 kcal/mol Å). The nonbonded interactions (electrostatic and van der Waals) cutoff is set to 10 Å while the dielectric constant $\epsilon$ in the gas phase is set to 79. Continuum solvation was implemented with Poisson Boltzmann Solver (PBF) and the PBF resolution was set to low. Single-point energy calculations were performed separately to determine the interaction energy ($\Delta E$) between the ligand and residue in the QM layer using the same level of theory as applied for the geometry optimization (Sladek et al., 2017).

## 2.5. In vitro biological assays

For the *in vitro* biological assays, a stock solution (10 mM) of the tested compound was prepared in DMSO. Six different concentrations (0.01-100 μM) were used in order to determine the $IC_{50}$ values of the tested compounds. The experiment was repeated following the same experimental conditions in six replicates and each time a duplicate was performed. The results are calculated from the mean of six different experiments, where the standard deviation did not exceed 10% ($\alpha = 0.01$).

### Inhibition of Soybean Lipoxygenase

The tested compound as stock solution (10 mM) was dissolved in DMSO. Aspartame and NDGA in a final concentration of 0.01-100 μM were incubated at room temperature with sodium linoleate (0.100 mL) and 0.2 mL of enzyme solution (1/$9 \times 10^{-4}$ w/v in saline) in buffer pH 9 (Tris) at room temperature (final volume 1 ml). The conversion of sodium linoleate to 13-hydroperoxylinoleic acid at 234 nm was recorded. The results were compared with the appropriate standard inhibitor NDGA. A blank control with the use of DMSO under the same experimental conditions was performed.

## 2.6. Saturation transfer difference (STD) NMR

NMR samples for STD experiments were prepared using 20 mM Tris buffer, pH = 7.2 in 99.9% $D_2O$. Firstly, aspartame was dissolved in 10 μL DMSO, and then Tris buffer pH = 7.2 in $D_2O$ was added, in a total volume of 600 μL. The concentration of the ligand aspartame in the NMR tube (600 μL) was 1 mM, whereas the concentration of the protein (soybean LOX-1) in the NMR tube was 0.02 mM, resulting in protein-ligand ratio of 1:50. Samples were subjected to STD experiments at 25 °C.

STD NMR experiments were recorded on Bruker AV 500 MHz spectrometer (Bruker Biospin, Rheinstetten, Germany) using the Topspin 2.1 suite. The spectral width was 6009.615 Hz. Pulse sequences provided in Bruker libraries of pulse programs were used. Relaxation delay was set to 1.5 s. Selective on-resonance irradiation frequency was set to 1.6 parts per million (ppm) with saturation time of 2 s. Selective saturation was achieved by a train of 50-ms Gauss-shaped pulses separated by a 2-ms delay. The duration of the presaturation of 2 s was adjusted using $n = 16$ cycles. Off-resonance irradiation frequency for the reference spectrum was applied at 20 ppm. Water suppression was achieved with excitation sculpting. Spectra were zero filled twice and the line broadening function of 1 Hz was applied. As far as the epitope mapping is concerned, the STD amplification factor was determined (Supporting Information, Section 3).

To investigate the interaction between soybean LOX-1 and aspartame, firstly, we recorded a proton ^{1}H NMR of the ligand in Tris buffer in $D_2O$, pH = 7.2, so as to have a complete assignment for the picture of aspartame. In a second step, the proper concentration of soybean LOX-1, which was

**Table 1.** Docking results of the natural sweeteners to LOX-1 (PDB ID: 5T5V).

| Natural Sweeteners | Binding affinity (kcal/mol) | Violations |
|---|---|---|
| Sorbitol | −8.6 | 1 Lipinski violation |
| Xylitol | −7.4 | 3 Ghose violations |
| Erythritol | −7.0 | 4 Ghose violation |
| Glycyrrhizin | – | 3 Lipinski violations |
| Glycerol | −4.6 | 4 Ghose violations |
| Mannitol | −8.8 | 1 Lipinski violation |
| Dextrose | −6.9 | 1 Lipinski violation |
| Maltitol | −11.5 | 2 Lipinski violations |
| Isomalt | −13.0 | 2 Lipinski violations |
| Tagatose | −7.6 | Low gastrointestinal absorption |
| Lactitol | −11.7 | 2 Lipinski violations |
| Maltose | −9.4 | 2 Lipinski violations |
| Galactose | −7.9 | Low gastrointestinal absorption |
| Trehalose | – | 2 Lipinski violations |
| Rebodioside | – | 3 Lipinski violations |
| Maltodextrin | – | 2 Lipinski violations |
| Monatin | – | Egan violation |
| Osladin | – | 3 Lipinski violations |
| D-psycose | −7.5 | 2 Ghose violations |
| Thaumatin | – | Lead-compound incompetence |
| Fructose | −6.8 | Low gastrointestinal absorption |
| Steviol | – | Lead-compound incompetence |
| Isomaltulose | −13.3 | 2 Lipinski violations |
| Lactulose | −11.4 | 2 Lipinski violations |

**Table 2.** Docking results of commercially available artificial sweeteners to LOX-1 (PDB ID: 5T5V).

| Artificial sweetener | XP GScore (kcal/mol) |
|---|---|
| Saccharin | −4.7 |
| Acesulfame potassium | −3.0 |
| Sucralose | −9.9 |
| Neohesperidindihydrochalcone | – |
| Sodium cyclamate | −5.1 |
| Mogroside_VV | – |
| Aspartame | −7.6 |
| Neotame | – |

estimated as 1:50 towards aspartame, was added to the aspartame solution and a proton $^1$H NMR spectrum was recorded, so as to select the desirable frequency related to the protein which will be saturated. In the next step, the STD NMR experiments were recorded, by saturating the protein at 804.314 Hz. The STD NMR experiment consists of two spectra: (a) an off-resonance spectrum where the frequency of saturation is moved away from the signals of the protein (20 ppm), so it has no effect to the binding affinity between the ligand and the protein; (b) an on-resonance spectrum where the protein is saturated in a specific frequency. These two spectra are automatically subtracted by the pulse sequence, to provide the STD spectrum (the difference spectrum), which is a result of the subtraction.

The intensity of the interaction between the aspartame protons and the protein, was determined through the STD amplification factor (Supporting Information, Section 3).

# 3. Results

## 3.1. In silico identification of potent LOX-1 binders

### 3.1.1. Natural sweeteners' docking studies to LOX-1
Induced Fit docking calculations have been applied to numerous available natural sweeteners so as to be assesed as potential anti-inflammatory agents. The docking results of all compounds to soybean LOX-1 is presented in Table 1 where they are ranked with the scoring function XP GScore that indicates the strength of ligand' s binding to the active site of the enzyme and takes into account the type of bond, the electrostatic, van der Waals and hydrophobic interactions created between the enzyme and the ligand during the formation of the complex. As illustrated in Table 1, numerous natural sweeteners bind strongly to LOX-1's active site (sorbitol, lactitol, isomalt), while others produce no poses in LOX's active site (maltodextrin, monatin, steviol). All natural

sweeteners were further evaluated by SwissADME tool (http://swissadme.ch./) (Daina et al., 2017) in order to predict their pharmacokinetics and drug-likeness properties. In the table below, the binding affinity of each natural sweetener in the active site of LOX-1 is presented, while the structural, pharmacokinetic and drug-likeness violations are pinpointed. It is evident that all natural sweeteners present important pharmacokinetic violations (mainly Lipinki and Ghose violations) (Ghose et al., 1999) and despite their high binding affinity to LOX enzyme, they are not compatible with establish drug-likeness criteria.

### 3.1.2. Artificial sweeteners' docking studies
The eight commercially available artificial sweeteners were screened as potent LOX-1 inhibitors. In silico docking studies indicated that among the tested compounds, aspartame and sucralose presented the strongest binding in the active site of the LOX-1 enzyme. The docking results of all eight compounds presented in Table 2 were ranked with the scoring function XP GScore. Sucralose and aspartame were further assessed by the SwissADME tool in order to predict their pharmacokinetic properties. From the two structures investigated, aspartame was superior in several pharmacokinetic and druglikeness properties in comparison to sucralose as it is demonstrated in Table S1.

## 3.2. Investigation of the stability of "LOX-1-aspartame" interaction

### 3.2.1. Docking calculations of aspartame to LOX-1
Induced fit docking (IFD), using Glide/XP algorithm, generated 17 conformers for aspartame docked in LOX-1 that were sorted based on decreasing IFDScore scoring function (Table S2) results, that takes into account not only the strength of ligand's binding to the protein's cavity, but also the Prime energy of the protein in all the protein-ligand complexes.

Conformer number 1 was chosen as the best docking pose in order to proceed to MD simulations. This conformation was chosen since it combines ligand's direct interaction with the Fe cation of the active site, while its low value of IFDScore (-1687.4 kcal/mol) indicates that the protein – ligand complex is the most stable compared to the others presented in Table S2. Moreover, both energetically and structurally, this cluster of conformers does not represent significant differences in their binding mode and any slight difference will converge within the process of MD simulation

and sampling to a mean protein-ligand structure. Emodel values that account for the various conformers were within a range of 7.85 as well as the XP GScore values differed only by 0.64 kcal/mol.

Aspartame in its best pose conformation (Figure 2) interacts strongly with the binding site of the protein. The strength of this binding is also related to the distances of the atoms participating in each interaction. These interactions, leading to the stabilization of the complex, include $\pi - \pi$ stacking between the indole group of Trp500 and the aromatic ring of aspartame (3.14 Å), the formation of two pi-cations between the amino group of aspartame and the two histidine residues of the active site, His499 and His504 (4.76 Å and 3.61 Å respectively) and the formation of a salt bridge between the Fe cation and the carboxyl group of the molecule (3.84 Å), which is better illustrated in Figure 2. The low binding energy in the cavity is also a result of the orientation of the lipophilic part of the molecule (aromatic ring and methyl ester) towards the hydrophobic residues of the cavity (i.e. Met497, Leu496, Cys492, Pro559, Phe557).

### 3.2.2. Molecular dynamics of the "LOX-1-aspartame" interaction

Molecular Dynamics simulations were conducted in order to evaluate the stability of aspartame's pose proposed by the docking studies. The MD simulation of the protein-ligand complex ($\Delta G_{bind}$=-7.6 kcal/mol) indicated aspartame's stable binding to LOX's cavity. To quantify this indication, the RMSD of the ligand was measured with respect to its docking pose coordinates. Throughout the simulation time (200 ns), aspartame is bound to LOX's binding site, while adopting a slightly different, more favorable, conformation than the one proposed by docking studies. Aspartame's stable binding in the cavity during the simulation time verifies our docking predictions and indicates that aspartame is indeed a strong LOX binder and a promising LOX inhibitor.

In Figure 3, the low RMSD value of protein's Ca atoms (<2.4 Å) indicates the good convergence of the system while the ligand RMSD is also presented for 200 ns of MD simulation time. The docking pose 1 was taken as reference-pose and the RMSD of ligand's heavy atoms was measured. The ligand's binding is considered quite stable since the RMSD value for the ligand is ∼0.9 Å during the whole simulation time as depicted in Figure 3. Further evaluation was conducted by computing the ligand's atoms' Root Mean Square Fluctuation (RMSF) presented in Figure S1. For most atoms, the RMSF values are as low as below 0.4 Å whereas all ligand's atoms have small fluctuations (lower than 0.4 Å). Molecular dynamics simulations were performed 3 times in order to investigate the reproducibility of the results stated above. The RMSD and RMSF values of both the protein and the ligand in all three simulations indicated the stability of the complex. The standard deviation of the RMSD values of the protein among the three simulations operated is 2.25 ± 0.2 Å, while the same value concerning the ligand is 0.85 ± 0.3 Å. The standard deviation of the RMSF value of the ligand fit on the protein between the three simulations is 1.0 ± 0.3 Å.

In order to further assess the stability of the binding pose, we performed cluster analysis on our MD trajectory based on the available ligand's conformations. Cluster analysis of the trajectory is a useful method for identifying, via statistical analysis, the most favored conformation that aspartame adopts during the simulation inside LOX's cavity. The trajectory was divided in 10 clusters of similar geometry based on ligand's conformations, using Desmond's algorithms and the cluster that was predominant for most of the simulation time, i.e. 27%, was chosen as the most relevant. Cluster analysis revealed important insights for aspartame's binding to LOX's active site. During the MD simulations, aspartame adopts a more favorable pose inside LOX's cavity and it is found to reside closer to the catalytic Fe cation in comparison with the docking pose (Figure S2). In particular, MD simulation is initiated with aspartame in spatial vicinity with catalytic Fe (3.84 Å), while we observe that in the predominant pose aspartame has approached the catalytic site and the distance between Fe and the carboxyl group of aspartame is measured 2.2 Å, as illustrated in Figure 4a. Furthermore, after the superposition of the two poses (docking pose and predominant cluster), we could observe that not only the carboxyl group of the molecule has been slightly displaced during MD simulation, but also the whole skeleton of aspartame has been displaced by approximately 3.01 Å (Figure 4a). Moreover, the conformation of aspartame does not heavily change during the whole time of the simulation, as illustrated by the superposition of all clusters derived by trajectory analysis (Figure 4b). These results corroborates the initial assumption that aspartame binds favorably to the active site of LOX-1 and remains stable inside the enzymatic cavity. Finally, in Figure 5c, we could observe that the active site of the protein has slightly changed during the MD simulation. In particular, the conformations of the residues in the active site present reduced but noticeable conformational changes, as well as the residues in the first coordination sphere of the catalytic iron. Hence, it is mandatory to perform further Quantum Mechanics/Molecular Mechanics (QM/MM) studies for the metalloprotein, in order to predict the most accurate configuration of the active site.

### 3.2.3. MM/GBSA calculations

MM/GBSA calculations have been applied to the statistically predominant "LOX-1-aspartame" complexes that derived from Desmond trajectory clustering. In the table below (Table 3), the binding energies of aspartame to soybean LOX-1 are illustrated. According to the $\Delta G_{bind}$ values that are presented in the table, aspartame binds favourably to the active site of soybean LOX-1 and in all the predominant clusters, the $\Delta G$ value is quite low. For the most prominent cluster (27% of the simulation time), $\Delta G_{bind}$ is calculated at −41.7 kcal/mol, while for cluster number 1 (21% of the simulation time) $\Delta G_{bind}$ value is quite lower (-54.8 Kcal/mol).

### 3.2.4. Qm/MM calculations on the LOX-aspartame interaction

In order to further evaluate the accuracy of the MD simulations and the credibility of the pose derived by classical mechanics calculations, we performed QM/MM studies for the "LOX-aspartame" complex. The active site of the protein
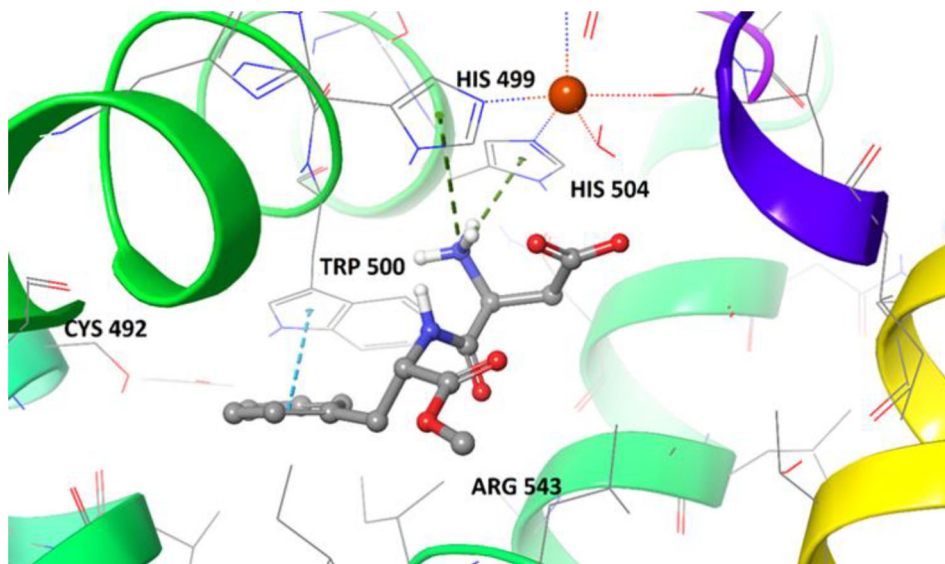
**Figure 2.** 3D pose of aspartame in LOX-1's active site. The Fe cation is represented in orange and the green and cyan dotted lines indicate aspartame's interactions with the active site's residues. Aspartame interacts with the cavity through π-π stacking between its aromatic ring and the indole ring of Trp500, while it forms pi-cation interactions between its charged amino group and the aromatic residues His499 and His504 of the active site.
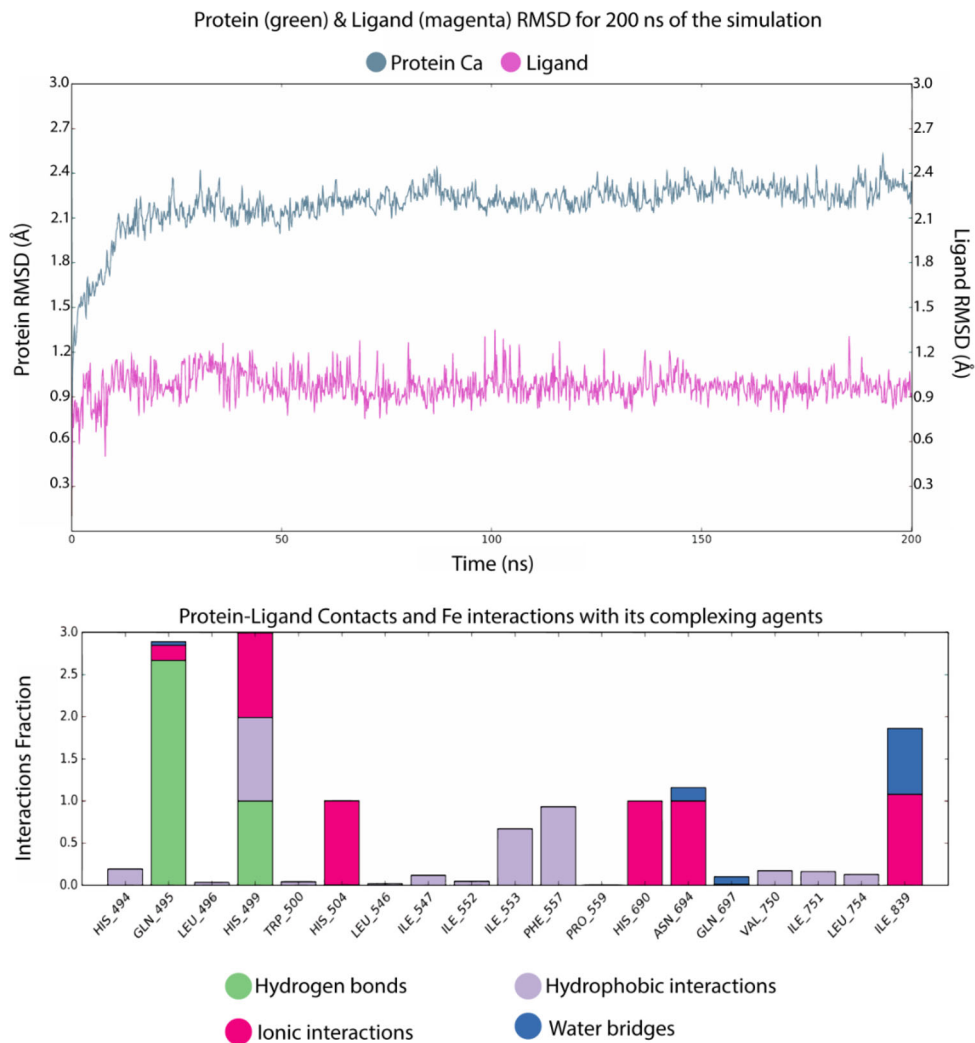


**Figure 3.** RMSD values of protein (green) and ligand (magenta) for 200 ns of the simulation taking as reference structure, the pose derived by docking studies (upper image). Protein-ligand contacts and Fe interaction with its complexing agents (lower image).

which is characterized by the Fe complex and aspartame, was geometrically optimized with QM calculations, while the rest of the protein is adiabatically minimized at each optimization step with MM methods. The initial pose of the QM
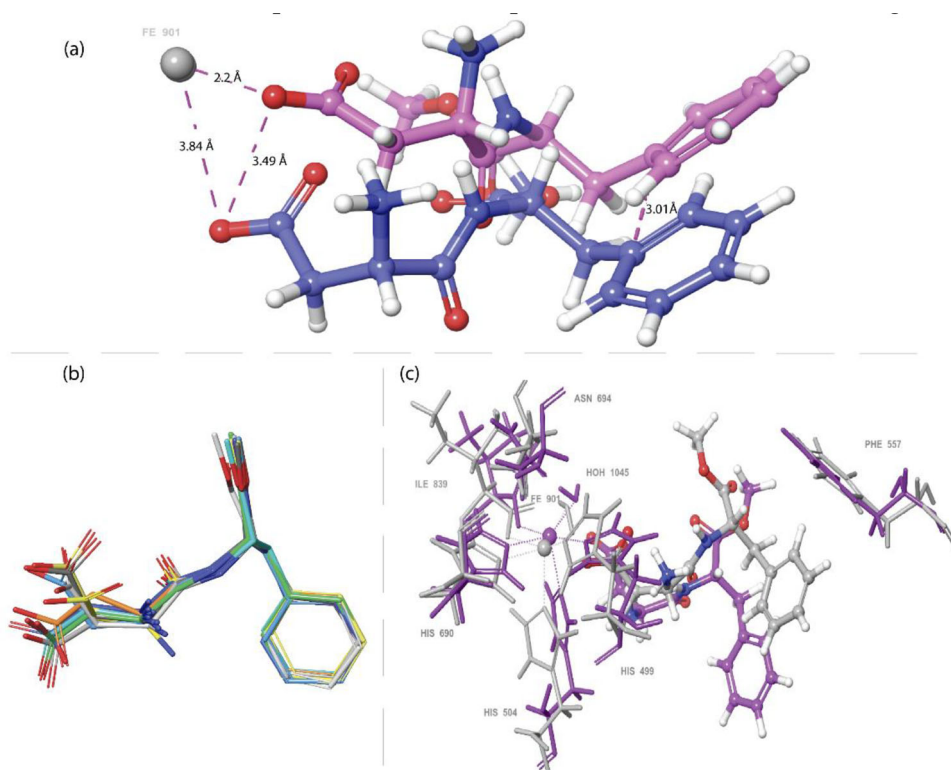
**Figure 4.** (a) Superposition of the Fe-aspartame complex derived from the docking studies (aspartame carrying blue skeleton) with the predominant cluster derived from MD simulations (aspartame carrying purple skeleton). Aspartame moves towards the catalytic Fe and slightly displaces during the simulation. (b). 10 conformations of aspartame derived from trajectory clustering aligned on the most stable conformation (yellow skeleton). (c). Superimposition of the active site as predicted by docking studies (purple colored) and by MD simulations (grey colored).
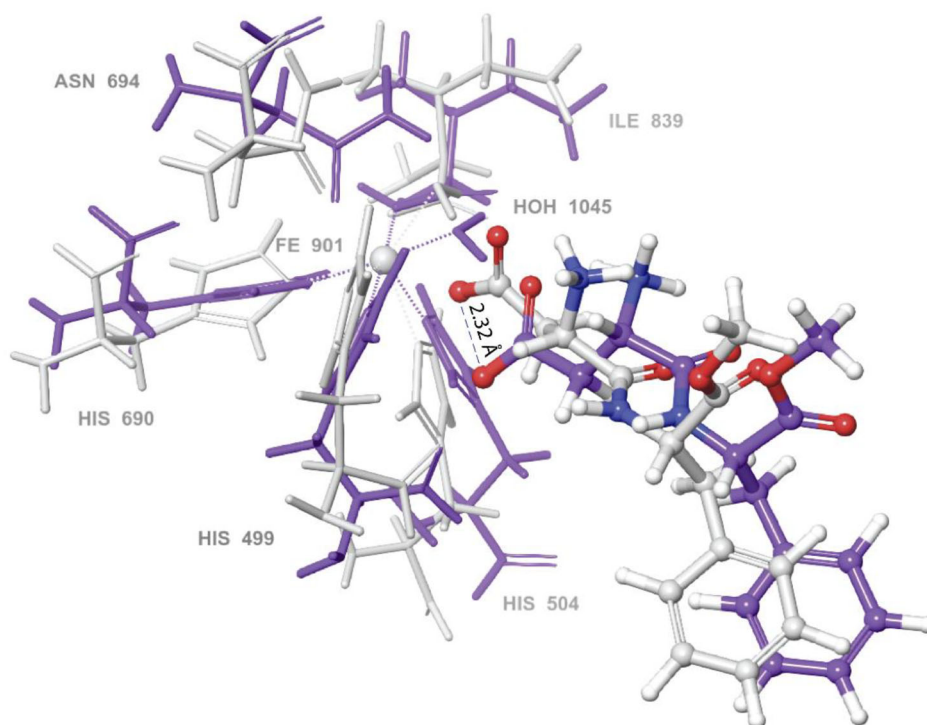


**Figure 5.** Superposition of the active site of the predominant cluster of aspartame (grey colored) and the pose derived by QM geometry optimization (purple colored).

optimization was the statistically predominant pose of MD studies that resulted in a more stable geometrical configuration. As illustrated in Figure 5, the conformation of the residues in iron's first coordination sphere have been slightly modified during QM optimization. In particular, the change of dihedral angles and bond lengths between Fe and its residue-ligands lead the complex to a more stable conformation. The bond length between Fe—OOC-Ile[839] has been

**Table 3.** $\Delta G_{bind}$ of LOX-1-aspartame complexes as calculated after MD studies.

| Cluster number | MM/GBSA $\Delta G_{bind}$ (kcal/mol) | Percentage of time during the simulation |
|---|---|---|
| 1 | −54.8 | 21% |
| 2 | −54.6 | 19% |
| 3 | −41.7 | 27% |

decreased from 2.28 Å to 1.95 Å, as well as the bond between Fe—HN-His[690] from 2.33 Å to 1.96 Å. The same effect is observed for the following bonds: Fe— HN-His[499] (from 2.36 Å to 1.99 Å), Fe— HN-His[504] (from 2.26 Å to 1.97 Å), Fe— HN-His[504] (from 2.26 Å to 1.97 Å), Fe— $H_2O^{1045}$ (from 2.13 Å to 1.93 Å) and Fe— OC-Asn[694] (from 2.16 Å to 1.93 Å). Besides the variations of the bond lengths, important conformational changes concerning the dihedral angles occur during QM optimization to the aforementioned histidine residues. In particular, His[690] flips its imidazole ring by approximately 60.6°, His[499] by 53.5° and His[504] by 52.2° with respect to their original conformations. Furthermore, aspartame moves slightly from its original position and the only conformational difference from the initial pose is the displacement of its carboxyl group 2.33 Å away from Fe cation (Figure 5). Consequently, the "LOX-aspartame" interaction predicted by all the implemented *in silico* studies proposed that aspartame enters LOX's cavity and adopts the same orientation in docking, MD and QM calculations. Hence, carboxyl group of the molecule is oriented towards catalytic Fe of the protein in all the different calculations performed. The accordance of QM calculations of the active site with the previously performed docking and MD studies reveals that all the parameters set to simulate the LOX-aspartame interaction potential are accurate and especially underlines the fact that OPLS2005 is a suitable forcefield for simulating the system under study.

### 3.2.5. *In vitro biological evaluation of the interaction of aspartame to LOX-1*

Having identified *in silico* the potential of aspartame to bind to LOX-1 we conducted further studies in order to verify its inhibition potential using relevant enzymatic assay. We found that aspartame presents high inhibitory activity compared to the reference compound nor-dihydroguaeretic acid (NDGA), a well-known lipoxygenase inhibitor, under the same experimental conditions (Table 4). The calculated $IC_{50}$ of aspartame due to its binding towards LOX-1 is quite high compared to other known strong LOX inhibitors (i.e. flavonoids, zileuton, BW 755 C) (Sostres et al., 2010).

### 3.2.6. *Charting aspartame - LOX-1 interaction through saturation transfer difference (STD) NMR experiments*

Having determined the potency of aspartame to inhibit LOX-1 we aimed to further probe its direct interaction as also to chart in atomic detail its epitope implicated in the recognition with the easily accessible soybean LOX-1. To evaluate the potential interaction of aspartame with LOX-1 we utilized Saturation Transfer Difference (STD) NMR (Mayer & Meyer, 2001). STD NMR not only probes the potential of a ligand to

**Table 4.** $IC_{50}$ values against LOX-1.

| Compounds | $IC_{50}$ (μM) ±SD* |
|---|---|
| Aspartame | 50 ± 3.0 |
| NDGA | 0.45 ± 0.013 |

The values are the mean of six replicates; *SD standard deviation.

interact with a potential pharmaceutical target, but also highlights the protons of the ligand that are implicated in the molecular interaction (Chatzikonstantinou et al., 2018). Recently, we successfully applied in cell STD NMR to probe intracellularly the interaction of a ligand with a cellular target. It is thus, a quite valuable tool to explore ligand-protein interactions.

The interaction between LOX-1 and aspartame, through STD NMR, is presented in Figure 6. As it can be seen from the difference spectrum, all the peaks which are related to the aromatic and aliphatic protons of aspartame, illustrate lower intensity than the ^{1}H-NMR reference spectrum. This result further confirms the interaction of aspartame with LOX-1.

The peak intensities can be integrated, in order to determine how close each proton is to the binding site of the receptor. According to calculations, the aromatic protons H-2 and H-4 interact with a percentage value of 38.26% with LOX-1, whereas the aromatic proton H-3 interacts with a value of 34.84%. Among all the aromatic protons, the highest percentage of interaction belongs to protons H-1 and H-5 with 44.34%, implying that these protons are closer to the binding site of the receptor.

In addition, for the aliphatic regions, the comparison between the ^{1}H NMR spectrum of the complex aspartame-soybean LOX-1 and the STD difference spectrum shows that all the aliphatic protons, as well as the aspartyl –$CH_3$ group interact with the binding site of the protein (Figure S3). The lower intensity of the peaks at the STD difference spectrum, compared to the reference Khanapure & Gordon Letts, 2004H proton spectrum, confirm that there is a binding interaction. According to calculations, the α-protons H-8, H-12a and H-12b near the two carboxylic groups interact successfully with the binding site of soybean LOX-1 with STD amplification factor values to be 20%. In addition, protons H-7a and H-7b, placed near the aromatic moiety interact with the protein with values of 12.72% and 30.44%, respectively. On the other hand, protons H-10a and H-10b placed between the two carbons bridging the amidic group bind sufficiently to the protein with values of 11.45% and 100% respectively, whereas proton H-11, which is located near the aminic group interacts at a percentage of 40.48%. H-11, thus, is closer to the binding site of the protein. Lastly, the $CH_3$ group which is part of the aspartyl moiety, also shows weak interaction with the binding site of the protein, with STD amplification factor value of 9.21% (Figure S4). The different STD amplification factors of the aspartame protons allow to chart its pharmacophore groups implicated in the binding. Previous studies concerning the inhibition of LOX-1 from flavonoids (Ribeiro et al., 2014), have shown that a catecholic moiety in the molecule could cause potent interaction with the active site of the enzyme. The number of the –OH
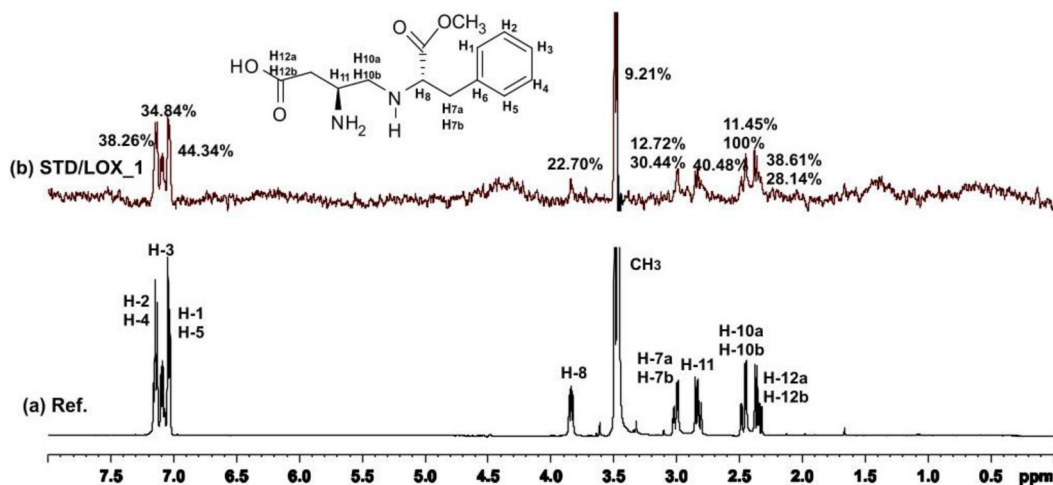
**Figure 6.** (a). $^1$H-NMR reference spectrum of aspartame (1 mM) containing the protein LOX-1 (0.02 mM), at 1:50 ratio towards aspartame, in buffer Tris pH = 7.2 and 600 μL D$_2$O at 500 MHz and 25 °C. (b). STD NMR difference spectrum of the complex aspartame-LOX-1, saturated in a frequency related to the protein (804.314 Hz) at 500 MHz and 25 °C. The strength of the interaction between the protons of aspartame and the binding site of LOX-1 is expressed through the respective percentages. The structure of aspartame is embedded in the top of the figure.

groups in the aromatic ring influences the potency of the inhibitory activity of a ligand. Flavonoids like luteolin, quercetin or taxifolin have been proven to be potent inhibitors of LOX-1, as they interact successfully with the active center of LOX-1. In addition, other flavonoids containing aromatic rings like curcumin and protocatechuic acid, have also been found to interact very efficiently with the active center of LOX-1, and, as a result they are potent LOX-1 inhibitors (Borbulevych et al., 2004). These data are in accordance to our findings indicating that the aromatic ring of the phenylalanine amino acid of aspartame interacts with LOX-1, through protons H-1 and H-5 pinpointing enhanced STD amplification factors. In addition, among other protons, which are part of the carbon chain, proton H-11 which is placed on the same carbon atom bearing the NH group, seems to be affected by the presence of hydrogen bonds, and, thus, it binds with efficient value to the binding site of LOX-1. Furthermore, aspartame seems to be planar in space, as its structure can be affected by the presence of the aromatic ring of phenylalanine, as well as the esteric moiety and the carboxylic group of the aspartic acid. This characteristic can also influence the strength of interaction between the enzyme and a possible ligand (Borbulevych et al., 2004).

The molecular profile of aspartame inside LOX-1's cavity proposed by STD NMR experiments is in accordance with the results derived from the *in silico* studies. As illustrated in Figure S2, depicting aspartame in LOX's cavity (predominant MD cluster), the aromatic ring (H1-H5) forms a π-π stacking interaction with Phe557, while the alkyl chain of the molecule (H10, H11, H12) carrying the carboxyl- and the amino-functional groups resides deep inside the cavity and interacts in the residues of the Fe-complex and Gln495.

### 3.3. In silico studies of aspartame to different LOX isoforms

After having identified aspartame as a promising binder to soybean LOX-1 using *in silico*, *in vitro* and STD NMR studies,

aspartame has been tested *in silico* for its potency to bind to other LOX isoforms. In order to conclude if aspartame could serve as a potential hit compound for designing novel anti-inflammatory drugs against LOX, it needs to be assessed for its binding to other organisms expressing the enzyme and mostly to mammals. Docking calculations and MD simulations have been implemented to different LOX isoforms. Table 5 presents the docking affinities of aspartame to LOXs' active sites, as well as it reports the compound's stability in each cavity as derived from the 200 ns of MD simulations.

According to the results derived from docking studies, aspartame presents high affinity to the active site of all LOX isoforms, as illustrated in the Table 5 (ΔG≤-7.6 kcal/mol). However, these results need to be further evaluated in order to assess if aspartame's strong binding to LOX cavity is an actual fact or just an artifact depicting only one snapshot of aspartame forced into the cavity. Herein, long MD simulations (∼200 ns) were conducted so as to predict aspartame's stability in each cavity, and the results are demonstrated in the right column of Table 5. RMSD values of the stable proteins' skeletons are presented in Figure S5, indicating the proper converge of the system and thus the accuracy of the results. LOX-3 exerts strong binding to aspartame and MD simulations indicated the stability of the formed complex. Furthermore, aspartame remains stable in human 5-LOX's cavity, which is an important result pointing aspartame as a promising anti-inflammatory drug targeting 5-LOX. Another "LOX-aspartame" complex in mammals that also remains quite stable is the one of rabbit organism (*Oryctolagus cuniculus*). In addition, aspartame forms unstable interactions in the rest of the LOX complexes, as it abandons the active sites of the enzymes and eventually the whole protein, and ends up in the aquatic environment of the solvent for most of the simulation time. These differences observed among LOX isoforms (formation of stable and unstable complexes) may be attributed to the structural differences among the enzyme's isoforms, including slight differences in the active site. Some of these proteins carry quite accessible to the solvent cavities, where aspartame could easily unbind from

**Table 5.** *In silico* studies of aspartame to different LOX isoforms.

| Enzyme | PDB ID | Organism | $\Delta G_{bind}$ (kcal/mol) | Complex stability |
|--------|--------|----------|------------------------------|-------------------|
| 13S-LOX | 5T5V | *Glycine max* | −7.6 | Stable |
| 5-LOX | 3O8Y | *Homo sapiens* | −8.5 | Stable |
| 15S-LOX | 1LOX | *Oryctolagus cuniculus* | −9.8 | Stable |
| 9S-LOX-3 | 1RRH | *Glycine max* | −7.9 | Stable |
| 12S-LOX | 3D3L | *Homo sapiens* | −10.0 | Unstable |
| 15-LOX | 4G32 | *Pseudomonas Aeruginosa* | −9.3 | Unstable |
| 12-LOX | 3RDE | *Sus scrofa* | −8.3 | Stable |
| 15-LOX-2 | 4NRE | *Homo sapiens* | −10.3 | Unstable |
| 13R-LOX | 5IR4 | *Pseudomonas Aeruginosa* | −9.4 | Unstable |

the active site and end up in the solvent area. Finally, all LOX isoforms derived from microorganisms do not seem to stabilize aspartame in their cavities in opposition to soybean isoforms that carry aspartame bound to their active sites throughout the whole simulation time. As far as human LOXs, two out of three different human isoforms could form stable aspartame's complexes. This finding could play an important role in the selectivity of aspartame as a potential drug molecule.

## 4. Discussion

Drug discovery is a very costly, tedious and time-consuming process. Along these lines we have initiated in our labs a process to discover potent bioactive compounds from food and beverage additives. This process could be of capital importance since such discovery could lead to orally bioavailable and safe drugs. Driven by our original hypothesis that potent LOX inhibitors could be identified from such sources, we screened natural and artificial sweeteners with the aid of *in silico* calculations. We discovered that aspartame is an orthosteric binder of LOX-1, which is a result verified with different computational and experimental methods. MD and QM/MM calculations predicted the most prominent conformation that aspartame adopts into the active site of LOX-1, as well as all the interactions aspartame forms with the residues in the cavity have been thoroughly evaluated. Electronic effects of the catalytic metallic active site were also taken into account, in order to improve the accuracy of our results. *In vitro* biological assays confirmed aspartame's binding to LOX enzyme and precisely calculated that aspartame exhibits $IC_{50}$ value of $50 \pm 3.0$ μM. This $IC_{50}$ value reveals that aspartame binds to LOX-1, although the strength of the binding needs to be further intensified. The molecular and atomic details of the binding were experimentally unveiled by STD NMR experiments and the results were in accordance with the proposed aspartame's conformation derived from the *in silico* studies. After having fully mapped the molecular details of aspartame's binding to LOX-1, further evaluation of the inhibitory properties of aspartame to other LOX isoforms has been conducted. Aspartame presents strong binding in 2 out of 3 different LOX isoforms of human organism, as unveiled by docking and MD studies. Thus, these discoveries reveal aspartame's inhibitory activity towards LOX enzyme and could pave the way to the structure derivatization of aspartame in order to produce stronger LOX binders and hence find numerous therapeutic applications against inflammation, cardiovascular diseases and cancer. From all the information acquired by this study, we conclude that aspartame is an important binder of LOX enzyme and it could serve as a hit for the design of novel, therapeutic agents. Furthermore, many compounds that have been identified as competent LOX-1 inhibitors, exhibit similar $IC_{50}$ values with this of aspartame. For instance, an investigation conducted by Katsori et al., revealed curcumin derivatives that exhibit inhibitory activity against LOX-1 ($IC_{50}=47$μM) (Katsori et al., 2011), while Yar's research group identified indolic compounds as LOX inhibitors with that exhibit $IC_{50}=53.1$ μM (Hu & Ma, 2018). In order to further evaluate the aspartame as a potent drug, the compound should be tested *in vitro* with human 15-LOX and 5-LOX isoforms. Herein, the results deriving from our current investigation indicate that since LOX-1 is implicated in the development of various inflammatory conditions, derivatization of aspartame will lead to important biologically active molecules targeting lipoxygenase isoforms and serve as potent drugs for the treatment of numerous inflammatory disorders and crucial diseases.

## ORCID

*Thomas Mavromoustakos* http://orcid.org/0000-0001-5309-992X

## References

Agulló, V., Domínguez-Perles, R., & García-Viguera, C. (2021). Sweetener influences plasma concentration of flavonoids in humans after an acute intake of a new (poly)phenol-rich beverage. *Nutrition, Metabolism, and Cardiovascular Diseases: NMCD*, *31*(3), 930–938. https://doi.org/10.1016/j.numecd.2020.11.016

Avis, I. M., Jett, M., Boyle, T., Vos, M. D., Moody, T., Treston, A. M., Martínez, A., & Mulshine, J. L. (1996). Growth control of lung cancer by interruption of 5-lipoxygenase-mediated growth factor signaling.

*The Journal of Clinical Investigation*, 97(3), 806–813. https://doi.org/10.1172/JCI118480

Banthiya, S., Kalms, J., Galemou Yoga, E., Ivanov, I., Carpena, X., Hamberg, M., Kuhn, H., & Scheerer, P. (2016). Structural and functional basis of phospholipid oxygenase activity of bacterial lipoxygenase from Pseudomonas aeruginosa. *Biochimica et Biophysica Acta*, 1861(11), 1681–1692. https://doi.org/10.1016/j.bbalip08.002.

Borbulevych, O. Y., Jankun, J., Selman, S. H., & Skrzypczak-Jankun, E. (2004). Lipoxygenase interactions with natural flavonoid, quercetin, reveal a complex with protocatechuic acid in its X-ray structure at 2.1 A resolution. *Proteins, Structure, Function, and genetics*, 54(1), 13–19. https://doi.org/10.1002/prot.10579

Boyington, J. C., Gaffney, B. J., & Amzel, L. M. (1990). Crystallization and preliminary X-ray analysis of soybean lipoxygenase-1, a non-heme iron-containing dioxygenase. *The Journal of Biological Chemistry*, 265(22), 12771–12773.

Brash, A. R. (1999). Lipoxygenases: Occurrence, functions, catalysis, and acquisition of substrate. *The Journal of Biological Chemistry*, 274(34), 23679–23682. https://doi.org/10.1074/jbc.274.34.23679

Carter, G. W., Young, P. R., Albert, D. H., Bouska, J., Dyer, R., Bell, R. L., Summers, J. B., & Brooks, D. W. (1991). 5-lipoxygenase inhibitory activity of zileuton. *The Journal of Pharmacology and Experimental Therapeutics*, 256(3), 929–937.

Catalano, A., & Procopio, A. (2005). New aspects on the role of lipoxygenases in cancer progression. *Histology and Histopathology*, 20(3), 969–975. https://doi.org/10.14670/HH-20.969

Chatzikonstantinou, A. V., Chatziathanasiadou, M. V., Ravera, E., Fragai, M., Parigi, G., Gerothanassis, I. P., Luchinat, C., Stamatis, H., & Tzakos, A. G. (2018). Enriching the biological space of natural products and charting drug metabolites, through real time biotransformation monitoring: The NMR tube bioreactor. *Biochimica et Biophysica Acta. General Subjects*, 1862(1), 1–8. https://doi.org/10.1016/j.bbagen.2017.09.021

Choi, J., Jae, K. C., Kim, S., & Shin, W. (2008). Conformational flexibility in mammalian 15S-lipoxygenase: Reinterpretation of the crystallographic data. *Proteins Struct Proteins*, 70(3), 1023–1032. https://doi.org/10.1002/prot.21590

Cicero, A. F. G., & Laghi, L. (2007). Activity and potential role of licofelone in the management of osteoarthritis. *Clinical Interventions in Aging*, 2(1), 73–79. https://doi.org/10.2147/ciia.2007.2.1.73

Claria, J., & Romano, M. (2005). Pharmacological intervention of cyclooxygenase-2 and 5-lipoxygenase pathways. Impact on inflammation and cancer. *Current Pharmaceutical Design*, 11(26), 3431–3447. https://doi.org/10.2174/138161205774370753

Daina, A., Michielin, O., & Zoete, V. (2017). SwissADME: A free web tool to evaluate pharmacokinetics, drug-likeness and medicinal chemistry friendliness of small molecules. *Scientific Reports*, 7, 42717. https://doi.org/10.1038/srep42717

Dobrian, A. D., Lieb, D. C., Cole, B. K., Taylor-Fishwick, D. A., Chakrabarti, S. K., & Nadler, J. L. (2011). Functional and pathological roles of the 12- and 15-lipoxygenases. *Progress in Lipid Research*, 50(1), 115–131. https://doi.org/10.1016/j.plipres.2010.10.005

Essmann, U., Perera, L., Berkowitz, M. L., Darden, T., Lee, H., & Pedersen, L. G. (1995). A smooth particle mesh Ewald method. *Journal of Chemical Physics*, 103(19), 8577–8593. https://doi.org/10.1063/1.470117

Feinmark, S. J., & Cornicelli, J. A. (1997). Is there a role for 15-lipoxygenase in atherogenesis? *Biochemical Pharmacology*, 54(9), 953–959. https://doi.org/10.1016/S0006-2952(97)00135-4

Flower, R. (2003). All the things that aspirin does. *BMJ (Clinical Research ed.)*, 327(7415), 572–573.

Garreta, A., Val-Moraes, S. P., García-Fernández, Q., Busquets, M., Juan, C., Oliver, A., Ortiz, A., Gaffney, B. J., Fita, I., Manresa, À., & Carpena, X. (2013). Structure and interaction with phospholipids of a prokaryotic lipoxygenase from Pseudomonas aeruginosa. *FASEB Journal: Official Publication of the Federation of American Societies for Experimental Biology*, 27(12), 4811–4821. https://doi.org/10.1096/fj.13-235952

Gheorghe, K. R., Korotkova, M., Catrina, A. I., Backman, L., af Klint, E., Claesson, H.-E., Rådmark, O., & Jakobsson, P.-J. (2009). Expression of 5-lipoxygenase and 15-lipoxygenase in rheumatoid arthritis synovium and effects of intraarticular glucocorticoids. *Arthritis Research & Therapy*, 11(3), R83. https://doi.org/10.1186/ar2717

Ghose, A. K., Viswanadhan, V. N., & Wendoloski, J. J. (1999). A knowledge-based approach in designing combinatorial or medicinal chemistry libraries for drug discovery. 1. A qualitative and quantitative characterization of known drug databases. *Journal of Combinatorial Chemistry*, 1(1), 55–68. https://doi.org/10.1021/cc9800071

Gilbert, N. C., Bartlett, S. G., Waight, M. T., Neau, D. B., Boeglin, W. E., Brash, A. R., & Newcomer, M. E. (2011). The structure of human 5-lipoxygenase. *Science (New York, N.Y.)*, 331(6014), 217–219. https://doi.org/10.1126/science.1197203

Gilbert, N. C., Gerstmeier, J., Schexnaydre, E. E., Börner, F., Garscha, U., Neau, D. B., Werz, O., & Newcomer, M. E. (2020). Structural and mechanistic insights into 5-lipoxygenase inhibition by natural products. *Nature Chemical Biology*, 16(7), 783–790. https://doi.org/10.1038/s41589-020-0544-7

Gillmor, S. A., Villaseñor, A., Fletterick, R., Sigal, E., & Browner, M. F. (1997). The structure of mammalian 15-lipoxygenase reveals similarity to the lipases and the determinants of substrate specificity. *Nature Structural Biology*, 4(12), 1003–1009. https://doi.org/10.1038/nsb1297-1003

Gupta, P., Tiwari, A., & Mishra, M. K. (2017). Taste masking of drugs: An extended approach. *International Journal of Current Advanced Research*, 6(3), 2571–2578. https://doi.org/10.24327/ijcar.2017.2578.0051

Haeggström, J. Z., & Funk, C. D. (2011). Lipoxygenase and leukotriene pathways: Biochemistry, biology, and roles in disease. *Chemical Reviews*, 111(10), 5866–5898. https://doi.org/10.1021/cr200246d

Hu, C., & Ma, S. (2018). Recent development of lipoxygenase inhibitors as anti-inflammatory agents. *Medchemcomm*, 9(2), 212–225. https://doi.org/10.1039/c7md00390k

Humphreys, D. D., Friesner, R. A., & Berne, B. J. (1994). A multiple-time-step Molecular Dynamics algorithm for macromolecules. *The Journal of Physical Chemistry*, 98(27), 6885–6892. https://doi.org/10.1021/j100078a035

Jorgensen, W. L., Maxwell, D. S., & Tirado-Rives, J. (1996). Development and testing of the OPLS all-atom force field on conformational energetics and properties of organic liquids. *Journal of the American Chemical Society*, 118(45), 11225–11236. https://doi.org/10.1021/ja9621760

Karatas, H., & Cakir-Aktas, C. (2019). 12/15 lipoxygenase as a therapeutic target in brain disorders. *Noro Psikiyatri Arsivi*, 56(4), 288–291. https://doi.org/10.29399/npa.23646

Katsori, A. M., Chatzopoulou, M., Dimas, K., Kontogiorgis, C., Patsilinakos, A., Trangas, T., & Hadjipavlou-Litina, D. (2011). Curcumin analogues as possible anti-proliferative & anti-inflammatory agents. *European Journal of Medicinal Chemistry*, 46(7), 2722–2735. https://doi.org/10.1016/j.ejmech.2011.03.060

Khanapure, S. P., & Gordon Letts, L. (2004). Perspectives and clinical significance of the biochemical and molecular pharmacology of eicosanoids. In *The Eicosanoids* (pp. 129–162). John Wiley &Sons.

Kobe, M. J., Neau, D. B., Mitchell, C. E., Bartlett, S. G., & Newcomer, M. E. (2014). The structure of human 15-lipoxygenase-2 with a substrate mimic. *The Journal of Biological Chemistry*, 289(12), 8562–8569. https://doi.org/10.1074/jbc.M113.543777

Lim, U. (2016). Artificial sweeteners and cancer - national cancer institute.

Lizunkova, P., Enuwosa, E., & Chichger, H. (2019). Activation of the sweet taste receptor T1R3 by sucralose attenuates VEGF-induced vasculogenesis in a cell model of the retinal microvascular endothelium. *Graefe's Archive for Clinical and Experimental Ophthalmology = Albrecht Von Graefes Archiv Fur Klinische Und Experimentelle Ophthalmologie*, 257(1), 71–81. https://doi.org/10.1007/s00417-018-4157-8

Lomelino, C. L., Murray, A. B., Supuran, C. T., & McKenna, R. (2018). Sweet Binders: Carbonic Anhydrase IX in Complex with Sucralose. *ACS Medicinal Chemistry Letters*, 9(7), 657–661. https://doi.org/10.1021/acsmedchemlett.8b00100

Luo, J., Chuang, T., Cheung, J., Quan, J., Tsai, J., Sullivan, C., Hector, R. F., Reed, M. J., Meszaros, K., King, S. R., Carlson, T. J., & Reaven, G. M. (1998). Masoprocol (nordihydroguaiaretic acid): A new antihyperglycemic agent isolated from the creosote bush (Larrea tridentata). *European Journal of Pharmacology*, 346(1), 77–79. https://doi.org/10.1016/S0014-2999(98)00139-3

Lyman, E., & Zuckerman, D. M. (2006). Ensemble-based convergence analysis of biomolecular trajectories. *Biophysical Journal*, 91(1), 164–172. https://doi.org/10.1529/biophysj.106.082941

Magnuson, B. A., Burdock, G. A., Doull, J., Kroes, R. M., Marsh, G. M., Pariza, M. W., Spencer, P. S., Waddell, W. J., Walker, R., & Williams, G. M. (2007). Aspartame: A safety evaluation based on current use levels, regulations, and toxicological and epidemiological studies. *Critical Reviews in Toxicology*, 37(8), 629–727. https://doi.org/10.1080/10408440701516184

Mahon, B. P., Hendon, A. M., Driscoll, J. M., Rankin, G. M., Poulsen, S. A., Supuran, C. T., & McKenna, R. (2015). Saccharin: A lead compound for structure-based drug design of carbonic anhydrase IX inhibitors. *Bioorganic & Medicinal Chemistry*, 23(4), 849–854. https://doi.org/10.1016/j.bmc.2014.12.030

Maillet, E. L., Cui, M., Jiang, P., Mezei, M., Hecht, E., Quijada, J., Margolskee, R. F., Osman, R., & Max, M. (2015). Characterization of the binding site of aspartame in the human sweet taste receptor. *Chemical Senses*, 40(8), 577–586. https://doi.org/10.1093/chemse/bjv045

Martyna, G. J., Tobias, D. J., & Klein, M. L. (1994). Constant pressure molecular dynamics algorithms. *Journal of Chemical Physics.*, 101(5), 4177–4189. https://doi.org/10.1063/1.467468

Mashima, R., & Okuyama, T. (2015). The role of lipoxygenases in pathophysiology; new insights and future perspectives. *Redox Biology*, 6, 297–310. https://doi.org/10.1016/j.redox.2015.08.006

Mayer, M., & Meyer, B. (2001). Group epitope mapping by saturation transfer difference NMR to identify segments of a ligand in direct contact with a protein receptor. *Journal of the American Chemical Society*, 123(25), 6108–6117. https://doi.org/10.1021/ja0100120

Murphy, R. C., & Gijon, M. A. (2007). Biosynthesis and metabolism of leukotrienes. *The Biochemical Journal*, 405(3), 379–395. https://doi.org/10.1042/BJ20070289

Murray, J. J., Tonnel, A. B., Brash, A. R., Roberts, L. J., Gosset, P., Workman, R., Capron, A., & Oates, J. A. (1986). Release of prostaglandin D2 into human airways during acute antigen challenge. *The New England Journal of Medicine*, 315(13), 800–804. https://doi.org/10.1056/nejm09253151304.

Offenbacher, A. R., Hu, S., Poss, E. M., Carr, C. A. M., Scouras, A. D., Prigozhin, D. M., Iavarone, A. T., Palla, A., Alber, T., Fraser, J. S., & Klinman, J. P. (2017). Hydrogen-Deuterium exchange of lipoxygenase uncovers a relationship between distal, solvent exposed protein motions and the thermal activation barrier for catalytic proton-coupled electron tunneling. *ACS Central Science*, 3(6), 570–579. https://doi.org/10.1021/acscentsci.7b00142

Oprea, T. I., Bauman, J. E., Bologa, C. G., Buranda, T., Chigaev, A., Edwards, B. S., Jarvik, J. W., Gresham, H. D., Haynes, M. K., Hjelle, B., Hromas, R., Hudson, L., Mackenzie, D. A., Muller, C. Y., Reed, J. C., Simons, P. C., Smagley, Y., Strouse, J., Survilladze, Z., … Sklar, L. A. (2011). Drug repurposing from an academic perspective. *Drug Discovery Today. Therapeutic Strategies*, 8(3-4), 61–69. https://doi.org/10.1016/j.ddstr.2011.10.002

Li, P., Wang, Z., Lam, S. M., & Shui, G. (2021). Rebaudioside a enhances resistance to oxidative stress and extends lifespan and healthspan in caenorhabditis elegans. *Antioxidants*, 10, 262. https://doi.org/10.3390/antiox10020262

Pattar, S. V., Adhoni, S. A., Kamanavalli, C. M., & Kumbar, S. S. (2020). In silico molecular docking studies and MM/GBSA analysis of coumarin-carbonodithioate hybrid derivatives divulge the anticancer potential against breast cancer. *Beni-Suef University Journal of Basic and Applied Sciences*, 9, 36-46. https://doi.org/10.1186/s43088-020-00059-7

Praticò, D., Zhukareva, V., Yao, Y., Uryu, K., Funk, C. D., Lawson, J. A., Trojanowski, J. Q., & Lee, V. M. Y. (2004). 12/15-Lipoxygenase is increased in Alzheimer's disease: possible involvement in brain oxidative stress. *The American Journal of Pathology*, 164(5), 1655–1662. https://doi.org/10.1016/S0002-9440(10)63724-8

Protein Data Bank. (2021). Protein Data Bank RCSB PDB: Homepage.

Rana, R., Sharma, R., & Kumar, A. (2019). Repurposing of fluvastatin against candida albicans CYP450 lanosterol 14 α-demethylase, a target enzyme for antifungal therapy: An in silico and in vitro study. *Current Molecular Medicine*, 19(7), 506–524. https://doi.org/10.2174/1566524019666190520094644

Ribeiro, D., Freitas, M., Tomé, S. M., Silva, A. M. S., Porto, G., Cabrita, E. J., Marques, M. M. B., & Fernandes, E. (2014). Inhibition of LOX by flavonoids: A structure-activity relationship study. *European Journal of Medicinal Chemistry*, 72, 137–145. https://doi.org/10.1016/j.ejmech.2013.11.030

Rioux, N., & Castonguay, A. (1998). Inhibitors of lipoxygenase: A new class of cancer chemopreventive agents. *Carcinogenesis*, 19(8), 1393–1400. https://doi.org/10.1093/carcin/19.8.1393

Rouzer, C. A., & Marnett, L. J. (2009). Cyclooxygenases: Structural and functional insights. *Journal of Lipid Research*, 50 Suppl, S29–S34. https://doi.org/10.1194/jlr.r800042-jlr200

Schrödinger LigPrep. (2018). Schrödinger. Schrödinger Release 2018–2.

Schrödinger LLC Prime. (2014). Schrödinger LLC Prime, version 3.5. New York.

Schrödinger LLC. (2011). Schrödinger Llc New York Ny Glide, version 5.7. Glid. Schrödinger LLC.

Schrödinger Maestro. (2018). Schrödinger. Schrödinger Release 2018–2.

Schrodinger, L.L.C. (2013). MacroModel, Version 10.2. New York.

Schrodinger. (2015). *Schrodinger software release 2015-2 induced fit docking*. Schrodinger Press.

Sharma, N., Singh, A., & Sharma, R. (2020). *Repurposing of auranofin against bacterial infections: An In silico and In vitro study*. Curr Comput Aided Drug Des.

Sherman, W., Day, T., Jacobson, M. P., Friesner, R. A., & Farid, R. (2006). Novel procedure for modeling ligand/receptor induced fit effects. *Journal of Medicinal Chemistry*, 49(2), 534–553. https://doi.org/10.1021/jm050540c

Skrzypczak-Jankun, E., Borbulevych, O. Y., Zavodszky, M. I., Baranski, M. R., Padmanabhan, K., Petricek, V., & Jankun, J. (2006). Effect of crystal freezing and small-molecule binding on internal cavity size in a large protein: X-ray and docking studies of lipoxygenase at ambient and low temperature at 2.0 A resolution. *Acta Crystallographica. Section D, Biological Crystallography*, 62(Pt 7), 766–775. https://doi.org/10.1107/S0907444906016982

Sladek, V., Kóňa, J., & Tokiwa, H. (2017). In silico analysis of interaction pattern switching in ligandreceptor binding in Golgi α-mannosidase II induced by the protonated states of inhibitors . *Physical Chemistry Chemical Physics : PCCP*, 19(19), 12527–12537. https://doi.org/10.1039/c7cp01200d

Sostres, C., Gargallo, C. J., Arroyo, M. T., & Lanas, A. (2010). Adverse effects of non-steroidal anti-inflammatory drugs (NSAIDs, aspirin and coxibs) on upper gastrointestinal tract. *Best Practice & Research. Clinical Gastroenterology*, 24(2), 121–132. https://doi.org/10.1016/j.bpg.2009.11.005

Tardif, J.-C., L'Allier, P. L., Ibrahim, R., Grégoire, J. C., Nozza, A., Cossette, M., Kouz, S., Lavoie, M.-A., Paquin, J., Brotz, T. M., Taub, R., & Pressacco, J. (2010). Treatment with 5-lipoxygenase inhibitor VIA-2291 (atreleuton) in patients with recent acute coronary syndrome.110.937169. *Circulation: Cardiovascular Imaging*, 3(3), 298–307. https://doi.org/10.1161/CIRCIMAGING

US Food & Drug Administration. (n.d.). US food & drug administration additional information about high-intensity sweeteners permitted for use in food in the United States.

Valentovic, M. Z. (2007). In xPharm: The comprehensive pharmacology reference.

Version, D.D. (2021). Version, D.D. Desmond Tutorial. Schroedinger., https://doi.org/10.1162/rest_a_00790

West, M., Mhatre, M., Ceballos, A., Floyd, R. A., Grammas, P., Gabbita, S. P., Hamdheydari, L., Mai, T., Mou, S., Pye, Q. N., Stewart, C., West, S., Williamson, K. S., Zemlan, F., & Hensley, K. (2004). The arachidonic acid 5-lipoxygenase inhibitor nordihydroguaiaretic acid inhibits tumor necrosis factor alpha activation of microglia and extends survival of G93A-SOD1 transgenic mice . *Journal of Neurochemistry*, 91(1), 133–143. https://doi.org/10.1111/j.1471-415902700.x.

Xu, S., Mueser, T. C., Marnett, L. J., & Funk, M. O. (2012). Crystal structure of 12-Lipoxygenase catalytic-domain-inhibitor complex identifies a substrate-binding channel for catalysis. *Structure (London, England : 1993)*, 20(9), 1490–1497. https://doi.org/10.1016/j.str.2012.06.003

Zhao, Y., Wang, W., Wang, Q., Zhang, X., & Ye, L. (2012). Lipid metabolism enzyme 5-LOX and its metabolite LTB4 are capable of activating transcription factor NF-κB in hepatoma cells. *Biochemical and Biophysical Research Communications*, 418(4), 647–651. https://doi.org/10.1016/j.bbrc.2012.01.068

Zuo, L., Christofi, F. L., Wright, V. P., Bao, S., & Clanton, T. L. (2004). Lipoxygenase-dependent superoxide release in skeletal muscle. *Journal of Applied Physiology (Bethesda, Md. : 1985)*, 97(2), 661–668. https://doi.org/10.1152/japplphysiol.00096.2004